

# Geography-Aware Large Language Models for Next POI Recommendation

Zhao Liu<sup>1</sup>, Wei Liu<sup>1</sup>, Huaijie Zhu<sup>1</sup>, Jianxing Yu<sup>1</sup>, Jian Yin<sup>1</sup>,  
Wang-Chien Lee<sup>2</sup>, Shun Wang<sup>1</sup>

<sup>1</sup>Sun Yat-sen University

<sup>2</sup>The Pennsylvania State University

{liuzh368, liuw259, zhuhuaijie, yujx26, issjyin, wangsh363}@mail.sysu.edu.cn,  
wlee@cse.psu.edu

## Abstract

The next Point-of-Interest (POI) recommendation task, aiming to predict users' next destination based on their historical movement data, plays a crucial role in location-based services and personalized applications. Accurate next POI recommendation relies heavily on modeling geographic information and POI transition relations, which are critical for capturing spatial dependencies and user movement patterns. While Large Language Models (LLMs) demonstrate strong semantic understanding and contextual modeling, their applications to spatial tasks such as the next POI recommendation face significant challenges: (1) the infrequent occurrence of specific GPS coordinates hinders effective and precise spatial context modeling, and (2) the lack of POI transition knowledge limits LLMs' understanding of potential POI-POI relationships. We therefore propose Geography-Aware Large Language Model (GA-LLM), a novel framework that enhances LLMs with two specialized modules: i) Geographic Coordinate Injection Module (GCIM) transforms GPS coordinates into meaningful spatial representations using a hierarchical and Fourier positional encoding, enabling GA-LLM to effectively capture geographic features with multiple granularities and perspectives. ii) POI Alignment Module (PAM) integrates POI transition relations into the LLM's semantic space, allowing it to infer global POI relationships and explore previously unseen POIs for users. Experiments on three datasets show the state-of-the-art performance of GA-LLM. The source code is available at: <https://anonymous.4open.science/r/GA-LLM-D2408>.

## 1 Introduction

Next Point-of-Interest (nPOI) recommendation, which aims to predict a user's next destination based on their historical movement data, plays a vital role in location-based services, enabling personalized applications such as tourism planning, restaurant discovery, and navigation. Traditional

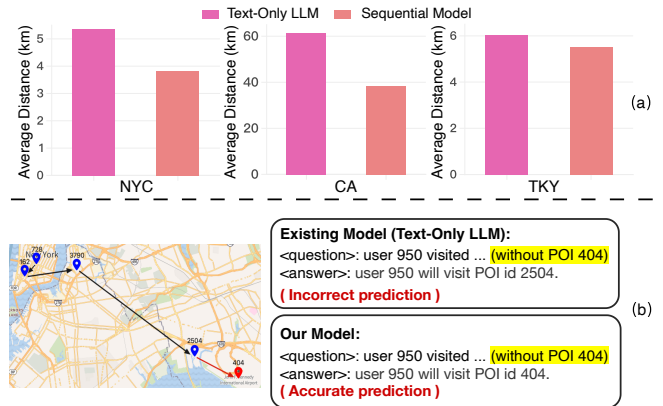


Figure 1: Illustration of text-only LLM limitations in POI recommendation. (a) Average error distances of incorrectly predicted POIs to their correct POIs for text-only LLMs versus sequential models on NYC, CA, and TKY datasets. (b) Case study where text-only LLM fails to predict POI 404 without input context, while our model leverages transition relations for accurate prediction.

nPOI recommendation methods, while effective in modeling user preferences through collaborative filtering [Rendle *et al.*, 2010] or graph-based approaches [Yan *et al.*, 2023; Yang *et al.*, 2022], often struggle to fully capture the semantic and contextual richness required for more complex and dynamic scenarios.

The rise of Large Language Models (LLMs), with their unparalleled ability to model sequential dependencies and understand contextual semantics, has opened up exciting new opportunities for significantly advancing nPOI recommendation tasks. By leveraging LLMs [Li *et al.*, 2024b], it becomes possible to bridge the gap between semantic modeling and diverse location-based data. Recent works [Tang *et al.*, 2024; Liao *et al.*, 2024; Li *et al.*, 2023] have shown the effectiveness of LLMs in recommendation tasks through their semantic understanding. However, applying LLMs to nPOI recommendation faces two key challenges.

**C1: Limited spatial awareness.** Existing methods [Li *et al.*, 2024b; Li *et al.*, 2023] often fail to capture spatial relationships, as LLMs are not inherently tailored to perceive geographic data like GPS coordinates [Balsebre *et al.*, 2024; Roberts *et al.*, 2023]. LLMs-based models may generate hal-

lucinated POIs far from the ground truth due to a lack of consideration for spatial proximity. As shown in Figure 1(a), text-only LLMs produce higher error distances in incorrect predictions compared to sequential models (e.g., ROTAN) on three datasets, underscoring their limitations in effectively capturing spatial dependencies. When humans visit lots of POIs with unique GPS coordinates, these coordinates are critical for distinguishing their complex affinities. However, minor variations and low occurrence frequencies of GPS coordinates hinder LLMs’ ability to model spatial relationships effectively. LLMs typically tokenize high-precision GPS coordinates, such as (40.8130989074707, -74.00180053710938), which have more than 10 decimal places. This process generates a large number of tokens (36 in this case), significantly escalating the computational cost and complicating the spatial relationship modeling.

**C2: Absence of POI transition relations.** Traditional LLM-based methods rely mainly on textual information. Beyond the semantic relation, users’ complete check-in trajectories hold rich potential POI transition knowledge. However, due to token limits in prompts, LLMs can only include couples of similar historical trajectories [Li *et al.*, 2024b], making it challenging to model sequential dynamics, especially when the ground truth POI is absent from the historical trajectories. As illustrated in Figure 1(b), when POI 404 (Kennedy Airport) is not explicitly mentioned in the input, a baseline LLM model predicts a previously mentioned POI 2504 (AirTrain JFK station) as the next destination, failing to infer POI 404 through the POI-POI transition pattern.

To address them, we propose the Geography-Aware Large Language Model (GA-LLM), integrating the Geographic Coordinate Injection Module (GCIM) and the Point-of-Interest Alignment Module (PAM). GCIM is designed to enhance the geographic awareness and adaptability of LLMs, transforming precise GPS coordinates into compact, efficient representations via hierarchical quadkey-based grid system, self-attention mechanisms and learnable Fourier transformations, respectively. PAM leverages global POI transition relationships, which can be extracted from sequential models [Zhang *et al.*, 2022; Lian *et al.*, 2020] or graph-based models [Feng *et al.*, 2024b; Huang *et al.*, 2024; Rao *et al.*, 2022], to align transition knowledge with the LLM’s semantic space.

In this work, we make the following contributions:

- We propose GA-LLM, a framework for next POI recommendation to mitigate hallucination issues of LLMs in spatial tasks. Especially, geographic coordinate injection module is designed to enhance the geographic awareness of LLMs.
- POI alignment module is proposed to incorporate POI transition relations into the semantic space of LLMs, enabling the model to capture sequential user movement patterns and address the limitations of text-only LLMs.
- Extensive experiments conducted on three public real-world datasets demonstrate that GA-LLM outperforms existing deep learning-based approaches and LLMs-based models in next POI recommendation tasks. Notably, it excels in addressing cold-start challenges and improving inference efficiency.

## 2 Related Work

### 2.1 Next POI Recommendation

Early work on next POI recommendation [Cheng *et al.*, 2013; He *et al.*, 2016] treats it as a sequential task using Markov chains and spatial constraints. With the rise of deep learning, RNN-based models gained popularity. HST-LSTM [Kong and Wu, 2018] incorporates spatial-temporal factors into LSTM gates, while LSTPM [Sun *et al.*, 2020] combines geodilated LSTM and non-local operations to model short-term preferences. STAN [Luo *et al.*, 2021] uses multimodal embeddings with bi-layer attention, and CFPRec [Zhang *et al.*, 2022] aligns multi-step planning with user preferences via attention. Graph-based methods advanced POI recommendation by modeling complex spatial-temporal relationships. GETNext [Yang *et al.*, 2022] enhances POI representations with trajectory flow maps, while STHGCN [Yan *et al.*, 2023] and SNPM [Yin *et al.*, 2023] leverage hypergraphs and dynamic neighbor graphs. ROTAN [Feng *et al.*, 2024b] uses rotation-based temporal attention, and MTNet [Huang *et al.*, 2024] models user preferences via mobility trees. However, these methods still face challenges in cold-start scenarios, particularly when there is limited user data, highlighting the need for more advanced models, such as LLMs, that are better suited to address these issues.

### 2.2 LLMs for Recommender Systems

Building on the success of LLMs in various domains [Radford *et al.*, 2021; Baeviski *et al.*, 2020], recent research [Wu *et al.*, 2024; Zhang *et al.*, 2023; Liu *et al.*, 2024] has explored their potential in recommender systems. Notable examples include GraphGPT [Tang *et al.*, 2024], aligning LLMs with graph-structured data via instruction tuning, and LLMRec [Wei *et al.*, 2024], augmenting interaction graphs with LLM-generated side information. For sequential recommendation, SeCor [Wang *et al.*, 2024] integrates semantic and collaborative embeddings, LLaRA [Liao *et al.*, 2024] employs hybrid prompting to align sequential user behavior, and ReLLa [Lin *et al.*, 2024] incorporates retrieval-based methods for long-sequence modeling. Semantic Convergence Framework [Li *et al.*, 2024a] maps sparse collaborative semantics like ItemIDs into LLMs’ dense token space to improve scalability. For next POI recommendation, LLM4POI [Li *et al.*, 2024b] uses trajectory prompting and key-query similarity to integrate heterogeneous LBSN data while addressing cold-start challenges. However, LLMs struggle with high-precision coordinates and fine-grained spatial relationships, limiting their application in location-based services. Our method incorporates spatial modeling and POI transitions to better handle geographic data and sequential dependencies.

## 3 Problem Definition

Next POI recommendation aims to predict the next location a user to visit based on their historical check-in records. Each check-in record is represented as a tuple  $q = (u, p, c, t, g)$ , where  $u$  represents a user,  $p$  denotes the POI,  $c$  is the POI category (e.g., restaurant, park),  $t$  is the timestamp, and  $g = (\alpha, \beta)$  specifies the geographic coordinates of the POI. Given the historical trajectory of a user  $u$ ,  $T_u(t) =$

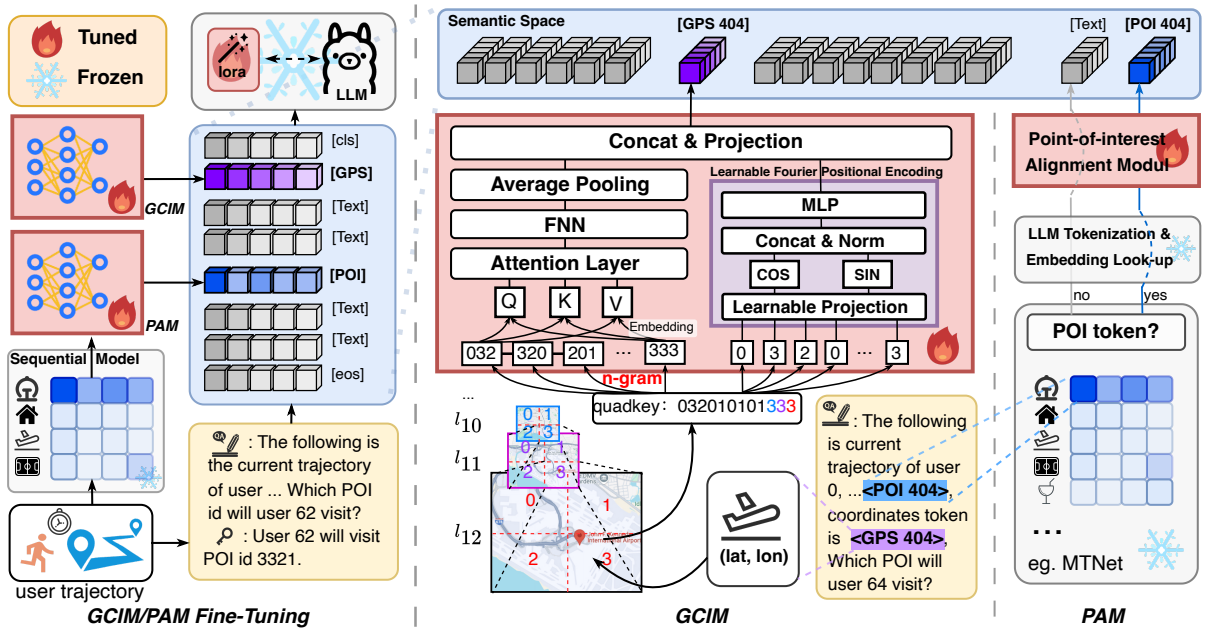


Figure 2: Overview of the GA-LLM framework. The left illustrates the workflow, where user trajectories are transformed into queries for LLM fine-tuning. The center highlights the GCIM module, encoding GPS data via a quadkey system and aligning it with the LLM’s semantic space. The right shows the PAM module, aligning POI embeddings from sequential models (e.g., MTNet) to the LLM’s semantic space.

$\{(p_1, c_1, t_1, g_1), \dots, (p_k, c_k, t_k, g_k)\}$  up to time  $t$ , the goal is to predict the next POI  $p_{k+1}$  that the user to visit at the subsequent timestamp  $t_{k+1}$ .

## 4 Methods

An idea for next POI recommendation is to leverage temporal and spatial trajectory information to model the likelihood of visiting candidate POIs. Accordingly, we propose the GA-LLM framework for this task.

### 4.1 The GA-LLM Framework

The GA-LLM framework, depicted in Figure 2, integrates spatial and semantic modeling to address challenges in next POI recommendation. It encodes user trajectory data into structured prompts for LLM fine-tuning. The framework features two key modules: the Geographic Coordinate Injection Module (GCIM), which transforms high-precision GPS data into spatial representations, and the Point-of-Interest Alignment Module (PAM), which aligns graph-based POI embeddings with the LLM’s semantic space. Together, these modules enable the model to effectively capture spatial dependencies, global relationships, and sequential patterns.

### 4.2 Geographic Coordinate Injection Module

GCIM processes latitude and longitude coordinates. While LLMmove [Feng *et al.*, 2024a] considers distance for POI recommendation, our approach incorporates finer spatial dependencies. As shown in the middle of Figure 2, GCIM maps GPS coordinates to hierarchical tiles using a unique Quadtree key (quadkey). It combines Fourier positional encoding with self-attention mechanisms to enrich quadkey representations,

which are integrated into the model’s input, allowing LLMs to capture spatial dependencies more effectively.

### Semantic Prompt Construction

We design structured prompts to encode POI details, including unique identifiers, categories, and geographic coordinates in a natural language format. For example:

“At  $[t]$ , user  $[u]$  visited  $p$ , represented as  $\langle \text{POI } [p] \rangle$ , with category  $[c]$ , located at  $\langle \text{GPS } [g] \rangle$ .”

GCIM processes  $\langle \text{GPS } [g] \rangle$  to produce spatial representations, while PAM projects  $\langle \text{POI } [p] \rangle$  into the LLM’s semantic space. This structured design effectively integrates spatial dependencies and POI-specific information, enhancing downstream task performance.

### Quadkey-Based Geographic Encoding

Inspired by the GeoEncoder proposed in GeoSAN [Lian *et al.*, 2020], we adopt a quadtree-based grid encoding scheme to transform latitude and longitude into compact spatial representations. Quadkeys uniquely identify grid tiles at varying resolution levels. At a specified zoom level  $l$ , the geographic space is projected into a 2D plane via the Mercator projection, mapping spherical coordinates  $(\alpha, \beta)$  into Cartesian coordinates  $(x, y)$  as follows:

$$x = \frac{\beta + 180}{360} \times 256 \times 2^l, \quad (1)$$

$$y = \left( \frac{1}{2} - \frac{1}{4\pi} \log \frac{1 + \sin(\alpha \cdot \pi/180)}{1 - \sin(\alpha \cdot \pi/180)} \right) \times 256 \times 2^l, \quad (2)$$

where,  $x$  and  $y$  are the positions of a GPS point on the grid at level  $l$ . Each tile is assigned a quadkey by encoding the grid divisions into a base-4 string, where the string length corresponds to the zoom level  $l$ . For a grid position, the resulting quadkey-derived representation  $S$  is defined as  $S = (s_1, s_2, \dots, s_L)$ , where  $L$  represents the number of hierarchical levels in the quadtree. Each  $s_i$  ( $i = 1, \dots, L$ ) denotes the digit at the  $i$ -th level of the quadkey encoding, capturing the spatial structure at progressively finer resolutions. This transformation discretizes continuous GPS coordinates into grid cells, ensuring nearby locations share similar quadkeys and reducing sparsity, while  $S$  encapsulates the hierarchical spatial information of the quadkey.

To enrich the representations, overlapping  $n$ -grams (e.g., {032, 320, 201, ...}) are generated from  $S$  to capture sequential patterns within the quadkey. Position encoding [Kang, 2018] is then added to the  $n$ -gram embeddings, producing position-enhanced representations. A self-attention mechanism is applied to emphasize critical spatial patterns across hierarchical quadkey sequences and is formally defined as:

$$\text{Attention}(Q, K, V) = \text{softmax} \left( \frac{QK^T}{\sqrt{d_k}} \right) V,$$

where  $Q, K, V$  are derived from the position-enhanced representations, and  $d_k$  is the dimensionality of the Key matrix. By dynamically assigning weights to  $n$ -grams, the self-attention mechanism captures both local spatial dependencies (from finer quadkeys) and global relationships (from coarser quadkeys), enhancing the model’s spatial representation.

### Learnable Fourier Positional Encoding

This Fourier-based encoding introduces periodic transformations to the model through the representation of  $S$ , enabling it to effectively capture fine-grained spatial patterns across multiple frequencies. By learning the projection matrix  $\mathbf{W}_s$ , the encoding adapts to the spatial structure of the quadkey representation, thereby refining embeddings for downstream tasks. Fourier encoding preserves high-frequency variations to capture subtle local changes, while low-frequency patterns reflect broader geographic trends, ensuring comprehensive spatial relationship representation.

Inspired by the learnable Fourier positional encoding approach proposed in [Li *et al.*, 2021], and building upon the methodology in [Zhang *et al.*, 2024], which applies Fourier embeddings directly to latitude and longitude, we adapt this technique to operate on quadkey-derived representations. Quadkeys better capture hierarchical spatial structures by discretizing geographic space into grid tiles. The Fourier-based geographic embedding  $\mathbf{F}(S)$  is computed as follows:

$$\mathbf{F}(S) = \frac{1}{\sqrt{M}} \left[ \cos(S \cdot \mathbf{W}_s^T) \parallel \sin(S \cdot \mathbf{W}_s^T) \right], \quad (3)$$

where  $S \in \mathbb{R}^L$  is the quadkey-derived grid position,  $M$  is the output embedding size,  $\mathbf{W}_s \in \mathbb{R}^{\frac{M}{2} \times L}$  is a learnable projection matrix initialized with a Gaussian distribution  $\mathbf{W}_s \sim N(0, \gamma^{-2})$ , and  $\gamma$  controls the spatial kernel width. The terms  $\cos(\cdot)$  and  $\sin(\cdot)$  denote element-wise cosine and sine functions, while  $\parallel$  represents concatenation.

The resulting Fourier-based geographic embeddings  $\mathbf{F}(S)$  are concatenated with the  $n$ -gram/self-attention representations discussed earlier. These enriched representations serve complementary purposes:  $n$ -gram/self-attention captures hierarchical and sequential dependencies within the quadkey structure, while Fourier encoding captures global spatial patterns through detailed frequency decomposition. This seamless integration effectively combines local and global spatial dependencies, equipping the model to process complex geographic relationships and optimize overall performance.

### 4.3 Point-of-Interest Alignment Module

While GCIM enhances the model’s spatial understanding by capturing geographic information, it does not fully address challenges posed by Point-of-Interest (POI) interactions, such as user transition preferences [Yin *et al.*, 2023]. These interactions are often modeled using graph-based methods [Yan *et al.*, 2023], which produce low-dimensional embeddings that are not directly compatible with the high-dimensional semantic space of LLMs. To address this, we introduce the Point-of-Interest Alignment Module (PAM), which aligns graph-based POI embeddings with the LLM’s semantic space. Unlike methods like E4SRec [Li *et al.*, 2023], which treat POIs as unique tokens and learn embeddings during fine-tuning, PAM bridges the gap between low-dimensional POI embeddings and the rich, contextual representations of LLMs, enabling the model to capture global relationships and user-specific behavioral patterns more effectively.

Specifically, PAM transforms POI embeddings generated by advanced graph-based models, such as MTNet [Huang *et al.*, 2024], STHGCN [Yan *et al.*, 2023], and ROTAN [Feng *et al.*, 2024b], into compatible high-dimensional representations. Formally, let  $e_i \in \mathbb{R}^d$  denote the low-dimensional embedding of the  $i$ -th POI. PAM maps  $e_i$  into the LLM’s semantic space through a multi-layer perceptron (MLP), thereby producing  $h_i \in \mathbb{R}^D$ . The alignment is formally defined as:

$$h = h_{\text{text}} \cup h_i, \quad h_i = \text{PAM}(e_i), \quad (4)$$

where  $h_{\text{text}}$  is the textual embedding derived from the LLM, and  $h \in \mathbb{R}^D$  combines textual and POI-specific information through concatenation. The MLP ensures that the POI embedding  $e_i$  is projected into a space that aligns with the LLM’s semantic features. Notably, GCIM (Section 4.2) follows a similar process, where spatial representations derived from quadkey-based grid positions are also projected into the LLM’s semantic space. This alignment ensures consistency between the POI-specific and spatial features, enabling a unified representation for downstream tasks.

By integrating spatial and transition-aware information into POI tokens, PAM enables the model to capture complex POI interactions, including user trajectories and movement preferences. Furthermore, when combined with the enriched spatial representations from GCIM, the unified feature representation allows the model to achieve a more comprehensive understanding of user behavior and spatial patterns, ultimately improving downstream task performance.

## 5 Experiments

In this section, we conduct extensive experiments on real-world datasets to evaluate the performance of the proposed GA-LLM by addressing the following research questions:

- **RQ1:** Does GA-LLM outperform baseline methods in next POI recommendation?
- **RQ2:** What is the impact of key components (GCIM and PAM) on the performance of GA-LLM?
- **RQ3:** How do geographic coordinates, mitigation of LLM hallucinations via spatial encoding, and the inclusion of GCIM in cross-city cold-start scenarios impact the performance of next POI recommendation models?
- **RQ4:** How does treating POIs as unique tokens versus a mapping layer affect transition relations, and how does PAM improve modeling POI transitions?
- **RQ5:** How does GA-LLM achieve computational efficiency during the training and inference stages?

### 5.1 Experimental Settings

**Datasets and Metrics.** We evaluate our approach on three datasets: Foursquare-NYC, Foursquare-TKY [Yang *et al.*, 2015], and Gowalla-CA [Cho *et al.*, 2011], summarized in Table 1. Foursquare-NYC and Foursquare-TKY focus on New York City and Tokyo, while Gowalla-CA spans regions in California and Nevada. Each dataset provides user check-ins annotated with POI ID, category, location, and timestamp. Following [Yan *et al.*, 2023], we remove POIs and users with fewer than 10 check-ins and split the data chronologically into 80% for training, 10% for validation, and 10% for testing. For evaluation, we use Top-1 Accuracy ( $Acc@1$ ), which calculates the proportion of cases where the top-ranked POI matches the ground truth, framing recommendation as a question-answering task under the "extreme position bias" setting [Li *et al.*, 2024b; Fairstein *et al.*, 2022].

Dataset	#user	#poi	#category	#check-in
NYC	1,048	4,981	318	103,941
TKY	2,282	7,833	290	405,000
CA	3,957	9,690	296	238,369

Table 1: Statistics of the three experimental datasets.

**Baselines.** Our experiments compare the proposed model with various baselines, including traditional methods like FPMC [Rendle *et al.*, 2010] and PRME [Feng *et al.*, 2015], recurrent models such as LSTM [Hochreiter and Schmidhuber, 1997], and advanced approaches incorporating spatiotemporal correlations, including STAN [Luo *et al.*, 2021] and PLSPL [Wu *et al.*, 2022]. Furthermore, we evaluate against graph-based methods like STGCN [Zhao *et al.*, 2022] and hypergraph-based approaches such as STHGCN [Yan *et al.*, 2023]. Transformer-based methods like GETNext [Yang *et al.*, 2022] and models addressing temporal dynamics, including ROTAN [Feng *et al.*, 2024b] and MTNet [Huang *et al.*, 2024], are also considered. While many LLM-based approaches use a yes/no question-answer setup, which does not

Model	NYC Acc@1	TKY Acc@1	CA Acc@1
FPMC	0.1003	0.0814	0.0383
LSTM	0.1305	0.1335	0.0665
PRME	0.1159	0.1052	0.0521
STGCN	0.1799	0.1716	0.0961
PLSPL	0.1917	0.1889	0.1072
STAN	0.2231	0.1963	0.1104
GETNext	0.2435	0.2254	0.1357
MTNext	0.2620	0.2575	0.1453
STHGCN	0.2734	0.2950	0.1730
ROTAN	0.3106	0.2458	0.2199
LLM4POI	<u>0.3372</u>	<u>0.3035</u>	0.2065
GA-LLM	<b>0.3919</b>	<b>0.3482</b>	<b>0.2566</b>
<i>Improv.</i>	16.19%	14.73%	16.69%

Table 2: Model performance. The overall best results are boldfaced, while the second-best results are underlined. Statistical significance testing shows that GA-LLM significantly outperforms the second-best baseline on all datasets, with  $p$ -value  $\leq 0.05$ .

align with our task, we choose LLM4POI [Li *et al.*, 2024b] as the baseline because it directly predicts specific POI IDs, thus matching our setup more effectively.

**Implementation Details.** We use Llama-2-7b-longlora-32k [Chen *et al.*, 2024; Touvron *et al.*, 2023] as our base model. Training uses a constant learning rate of  $2 \times 10^{-5}$ , with 20 warm-up steps, no weight decay, and a batch size of 1 per GPU. The maximum sequence length is set to 32,768 tokens, and each dataset is fine-tuned for 3 epochs. All experiments run on servers equipped with Nvidia A800 GPUs.

### 5.2 Main Results (RQ1)

We compare the performance of GA-LLM with various baselines on three datasets, as shown in Table 2. GA-LLM achieves significant improvements in  $Acc@1$ , surpassing the best baselines by 16.19%, 14.73%, and 16.69% on the NYC, TKY, and CA datasets, respectively. These results highlight GA-LLM’s ability to model diverse scenarios, from NYC’s smaller and more structured dataset to CA’s broader geographical coverage with higher data sparsity. Notably, while the improvement on the CA dataset over the best baseline ROTAN is 16.69%, it is worth paying attention to LLM4POI, which also exploits an LLM like GA-LLM dose. As Shown, GA-LLM achieves a much larger improvement of 24.26% over LLM4POI. This demonstrates GA-LLM’s effectiveness in overcoming the inherent limitations of text-only LLMs by incorporating geographic and POI-specific embeddings, which significantly enhance its ability to handle geographically extensive datasets with sparse spatial distributions. These findings underscore the strength of integrating spatial-temporal patterns and contextual relationships into the LLM framework, making GA-LLM particularly robust and adaptable for next POI recommendation tasks.

### 5.3 Ablation Study (RQ2)

To evaluate the impact of key components, we compare the performance of the full GA-LLM model, GA-LLM without

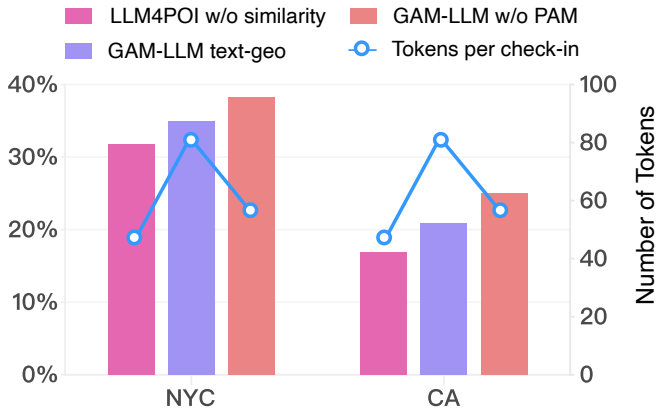


Figure 3: Comparison of methods handling geographic coordinates.

Model	NYC Acc@1	TKY Acc@1	CA Acc@1
Full Model	<b>0.3919</b>	<b>0.3482</b>	<b>0.2566</b>
w/o GCIM	0.3729	0.3370	0.2402
w/o Fourier	0.3800	0.3435	0.2467
w/o PAM	0.3826	0.3429	0.2499

Table 3: Ablation study results on NYC, TKY, and CA datasets.

GCIM, GA-LLM without PAM, and GA-LLM without the learnable Fourier transformation (w/o Fourier) across NYC, TKY, and CA datasets. As shown in Table 3, removing GCIM causes noticeable drops, particularly on datasets where spatial relationships are critical. Similarly, excluding PAM reduces accuracy across all datasets, highlighting its role in capturing POI transition relations. The ablation of the learnable Fourier transformation, a key component of GCIM, also results in performance degradation, demonstrating its importance in refining spatial representations.

#### 5.4 Geographic Information Analysis (RQ3)

Geographic information is essential for next POI recommendation, addressing challenges in spatial modeling and cross-city cold-start scenarios. This section evaluates GA-LLM across three aspects: (1) geographic coordinates’ role in recommendation performance, (2) spatial encoding’s impact on reducing errors and LLM hallucinations, and (3) GCIM’s cross-city generalization capability.

**Geographic Coordinates in POI Recommendation.** We compare three methods of incorporating geographic information: (i) LLM4POI w/o similarity, excluding similar trajectories; (ii) GA-LLM text-geo, expressing geographic data as textual descriptions (e.g., “northwest 2.3 km from the previous POI”), increasing tokens; and (iii) GA-LLM w/o PAM, encoding latitude and longitude into compact representations via GCIM, avoiding verbose descriptions. As shown in Figure 3, incorporating geographic information improves performance across all methods. GA-LLM w/o PAM achieves higher accuracy with fewer tokens, demonstrating GCIM’s efficiency and scalability for next POI recommendation.

**Mitigating LLM Hallucinations via Spatial Encoding.**

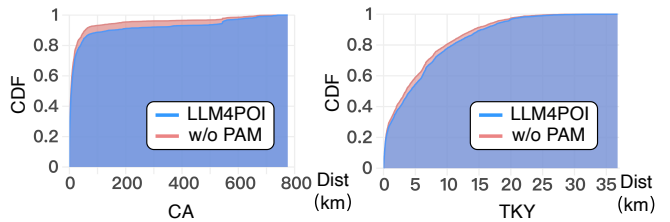


Figure 4: Cumulative distribution function (CDF) of distances between incorrectly predicted and ground truth POIs on two datasets.

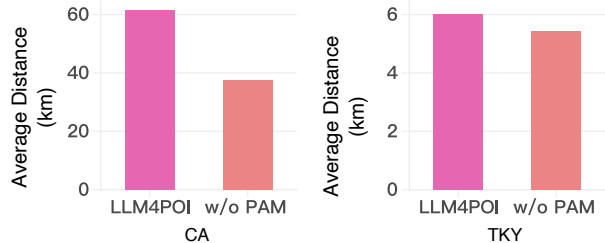


Figure 5: Average error distances between incorrectly predicted and ground truth POIs on CA and TKY.

Figures 4 and 5 demonstrate GCIM’s impact on reducing geographically implausible predictions. Figure 4 shows the CDF of error distances between predicted POIs and the ground truth, where GA-LLM w/o PAM results in smaller distances than LLM4POI. Figure 5 illustrates this with average distances reduced from 61.38 km to 37.63 km in the CA dataset. These results highlight GCIM’s ability to constrain prediction errors to plausible regions, effectively mitigating LLM hallucinations, especially in sparse datasets like CA.

**Cross-City Cold-Start Analysis.** Our GCIM module, a plug-in component of GA-LLM, enables effective integration of geographic information in cross-city cold-start scenarios. In this setting, a model trained on one city predicts POIs in another, a key challenge in location-based services. As shown in Table 4, GA-LLM w/o PAM outperforms LLM4POI, achieving significant improvement in  $Acc@1$  for cross-city tasks. These results demonstrate GCIM’s ability to capture global geographic patterns and generalize across regions by emphasizing global features over local dependencies. Notably, performance for training on TKY and testing on NYC surpasses training and testing on NYC, due to TKY’s richer geographic

Model	Trained on	NYC Acc@1	TKY Acc@1	CA Acc@1
LLM4POI	NYC	0.3372	0.2594	0.1885
	TKY	0.3463	0.3035	0.1960
	CA	0.3344	0.2600	0.2065
w/o PAM	NYC	0.3826	0.3018	0.2053
	TKY	0.4059	0.3429	0.2273
	CA	0.3670	0.3065	0.2499

Table 4: The models are LLM4POI and GA-LLM w/o PAM trained on one of the NYC, TKY, and CA datasets and evaluated on the rest.

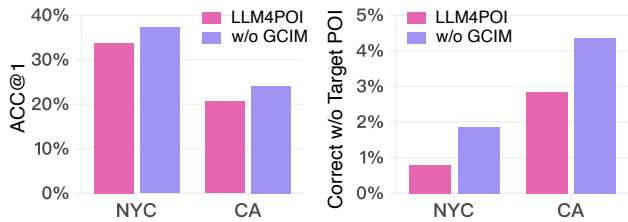


Figure 6: Proportion of successful predictions where the target POI does not appear in the input question, for LLM4POI and GA-LLM w/o GCIM across NYC and CA datasets.

Model	NYC	CA
	Acc@1	Acc@1
LLM4POI	0.3372	0.2065
token-based	0.3389	0.2226
w/o GCIM	<b>0.3729</b>	<b>0.2402</b>

Table 5: Performance comparison between token-based POI representation and our PAM-based approach.

diversity compared to NYC’s denser POI distribution.

### 5.5 Sequential Transition Modeling (RQ4)

This section analyzes the effectiveness of the Point-of-Interest Alignment Module (PAM) in capturing POI transition relations. The analysis is divided into two parts: (1) evaluating the strategy of treating POIs as new tokens and its limitations, and (2) demonstrating the benefits of PAM in improving accuracy and capturing transition relations.

**Evaluating POI Tokens and Transition Injection.** We compare our approach to E4SRec [Li *et al.*, 2023], which treats each POI as a unique token in the vocabulary, initializing POI embeddings with pre-trained representations from MTNet and fine-tuning during training. In contrast, our PAM-based method employs a projector layer during LLM fine-tuning to align POI representations with the LLM’s semantic space, avoiding reliance on individual POI-specific embeddings. As shown in Table 5, the token-based approach performs better in CA, likely due to traditional POI embeddings capturing transition relations in sparse datasets. However, it struggles in NYC, where the higher density and proximity of POIs make distinguishing embeddings during initialization challenging. This highlights a limitation of the tokenization strategy in dense urban environments. In contrast, our PAM-based approach overcomes these challenges by leveraging semantic mappings to model transition relations, delivering consistently strong performance across datasets.

**Effectiveness of Transition Preference Injection.** Capturing POI transition relations is critical for predicting target POIs that do not explicitly appear in the input question. In the test datasets, 75.8% of target POIs in NYC, 73.5% in TKY, and 55.6% in CA appear in the input question. Text-only LLMs like LLM4POI rely heavily on the presence of the target POI in the input, limiting performance when this context is missing. Our PAM module addresses this limitation by capturing transition relations through contextualized embeddings. As shown in Figure 6, PAM improves the correct

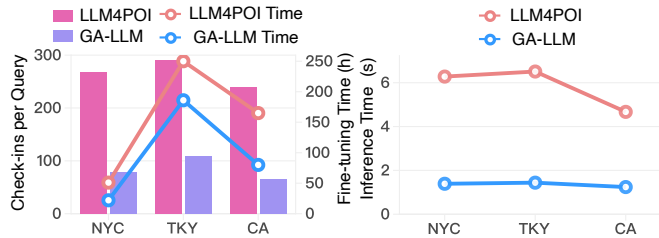


Figure 7: Efficiency analysis of GA-LLM and LLM4POI. Left: Fine-tuning time and average check-ins per query. Right: Per-query inference time across datasets.

predictions where the target POI is absent from the input, increasing ACC@1 from 2.85% to 4.36% in CA, demonstrating its effectiveness. Furthermore, PAM is a flexible and generalizable component compatible with various sequential models. While our experiments use MTNet, additional results on other models in the supplementary materials demonstrate its adaptability across scenarios.

### 5.6 Model Efficiency Study (RQ5)

The study evaluates the computational efficiency of GA-LLM during training and inference stages, compared to LLM4POI. **Training Efficiency Analysis.** The left side of Figure 7 compares the training efficiency of GA-LLM and LLM4POI, where LLM4POI uses 200 historical check-ins per query. GA-LLM achieves shorter fine-tuning times across datasets by processing fewer check-ins, reducing token consumption. For fairness, we focus solely on the final fine-tuning stage, excluding pre-training for GCIM and PAM.

**Inference Efficiency Analysis.** The right side of Figure 7 shows that GA-LLM achieves faster inference time per query than LLM4POI, primarily due to processing fewer check-ins per query. The components in GA-LLM, i.e., GCIM and PAM, introduce minimal overhead, ensuring both efficient inference and consistently high accuracy.

## 6 Conclusion

In this paper, we propose GA-LLM, a framework that integrates geographic and sequential transition modeling into large language models for next POI recommendation. In GA-LLM, the Geographic Coordinate Injection Module (GCIM) converts precise GPS data into compact spatial representations, capturing geographic patterns across multiple granularities and perspectives. The Point-of-Interest Alignment Module (PAM) models POI transition relations, leveraging contextual embeddings to address text-only LLM limitations on exploring unvisited POIs. Extensive experiments confirm the effectiveness and efficiency of integrating geography-aware representations, POI transition knowledge and the semantic understanding capabilities of LLMs. While GA-LLM shows strong performance in accuracy and adaptability across datasets, challenges remain in sparse datasets and evolving user behaviors. Future work is planned to align user behavior modalities, such as visit times, into the LLMs’ semantic space to further enhance geographic understanding and user preferences.

## References

- [Baevski *et al.*, 2020] Alexei Baevski, Yuhao Zhou, Abdelrahman Mohamed, and Michael Auli. wav2vec 2.0: A framework for self-supervised learning of speech representations. In *NeurIPS*, 2020.
- [Balsebre *et al.*, 2024] Pasquale Balsebre, Weiming Huang, Gao Cong, and Yi Li. City foundation models for learning general purpose representations from openstreetmap. In *CIKM*, pages 87–97. ACM, 2024.
- [Chen *et al.*, 2024] Yukang Chen, Shengju Qian, Haotian Tang, Xin Lai, Zhijian Liu, Song Han, and Jiaya Jia. Longlora: Efficient fine-tuning of long-context large language models. In *ICLR*. OpenReview.net, 2024.
- [Cheng *et al.*, 2013] Chen Cheng, Haiqin Yang, Michael R. Lyu, and Irwin King. Where you like to go next: Successful point-of-interest recommendation. In *IJCAI*, pages 2605–2611. IJCAI/AAAI, 2013.
- [Cho *et al.*, 2011] Eunjoon Cho, Seth A. Myers, and Jure Leskovec. Friendship and mobility: user movement in location-based social networks. In *Proceedings of the 17th ACM SIGKDD International Conference on Knowledge Discovery and Data Mining*, pages 1082–1090. ACM, 2011.
- [Fairstein *et al.*, 2022] Yaron Fairstein, Elad Haramaty, Arnon Lazerson, and Liane Lewin-Eytan. External evaluation of ranking models under extreme position-bias. In *WSDM '22: The Fifteenth ACM International Conference on Web Search and Data Mining*, pages 252–261. ACM, 2022.
- [Feng *et al.*, 2015] Shanshan Feng, Xutao Li, Yifeng Zeng, Gao Cong, Yeow Meng Chee, and Quan Yuan. Personalized ranking metric embedding for next new POI recommendation. In *IJCAI*, pages 2069–2075. AAAI Press, 2015.
- [Feng *et al.*, 2024a] Shanshan Feng, Haoming Lyu, Caishun Chen, and Yew-Soon Ong. Where to move next: Zero-shot generalization of llms for next poi recommendation, 2024.
- [Feng *et al.*, 2024b] Shanshan Feng, Feiyu Meng, Lisi Chen, Shuo Shang, and Yew Soon Ong. ROTAN: A rotation-based temporal attention network for time-specific next POI recommendation. In *Proceedings of the 30th ACM SIGKDD Conference on Knowledge Discovery and Data Mining*, pages 759–770. ACM, 2024.
- [He *et al.*, 2016] Jing He, Xin Li, Lejian Liao, Dandan Song, and William K. Cheung. Inferring a personalized next point-of-interest recommendation model with latent behavior patterns. In *Proceedings of the Thirtieth AAAI Conference on Artificial Intelligence*, pages 137–143. AAAI Press, 2016.
- [Hochreiter and Schmidhuber, 1997] Sepp Hochreiter and Jürgen Schmidhuber. Long short-term memory. *Neural Comput.*, 9(8):1735–1780, 1997.
- [Huang *et al.*, 2024] Tianhao Huang, Xuan Pan, Xiangrui Cai, Ying Zhang, and Xiaojie Yuan. Learning time slot preferences via mobility tree for next POI recommendation. In *Thirty-Eighth AAAI Conference on Artificial Intelligence*, pages 8535–8543. AAAI Press, 2024.
- [Kang, 2018] Wang-Cheng Kang. Self-attentive sequential recommendation. In *ICDM*, pages 197–206. IEEE Computer Society, 2018.
- [Kong and Wu, 2018] Dejiang Kong and Fei Wu. HST-LSTM: A hierarchical spatial-temporal long-short term memory network for location prediction. In *IJCAI*, pages 2341–2347. ijcai.org, 2018.
- [Li *et al.*, 2021] Yang Li, Si Si, Gang Li, Cho-Jui Hsieh, and Samy Bengio. Learnable fourier features for multi-dimensional spatial positional encoding. In *NeurIPS*, pages 15816–15829, 2021.
- [Li *et al.*, 2023] Xinhang Li, Chong Chen, Xiangyu Zhao, Yong Zhang, and Chunxiao Xing. E4srec: An elegant effective efficient extensible solution of large language models for sequential recommendation. *CoRR*, abs/2312.02443, 2023.
- [Li *et al.*, 2024a] Guanghan Li, Xun Zhang, Yufei Zhang, Yifan Yin, Guojun Yin, and Wei Lin. Semantic convergence: Harmonizing recommender systems via two-stage alignment and behavioral semantic tokenization, 2024.
- [Li *et al.*, 2024b] Peibo Li, Maarten de Rijke, Hao Xue, Shuang Ao, Yang Song, and Flora D. Salim. Large language models for next point-of-interest recommendation. In *SIGIR*, pages 1463–1472. ACM, 2024.
- [Lian *et al.*, 2020] Defu Lian, Yongji Wu, Yong Ge, Xing Xie, and Enhong Chen. Geography-aware sequential location recommendation. In *The 26th ACM SIGKDD Conference on Knowledge Discovery and Data Mining*, pages 2009–2019. ACM, 2020.
- [Liao *et al.*, 2024] Jiayi Liao, Sihang Li, Zhengyi Yang, Jiancan Wu, Yancheng Yuan, Xiang Wang, and Xiangnan He. Llora: Large language-recommendation assistant. In *SIGIR*, pages 1785–1795. ACM, 2024.
- [Lin *et al.*, 2024] Jianghao Lin, Rong Shan, Chenxu Zhu, Kounianhua Du, Bo Chen, Shigang Quan, Ruiming Tang, Yong Yu, and Weinan Zhang. Rella: Retrieval-enhanced large language models for lifelong sequential behavior comprehension in recommendation. In *Proceedings of the ACM on Web Conference 2024*, pages 3497–3508. ACM, 2024.
- [Liu *et al.*, 2024] Qidong Liu, Xian Wu, Xiangyu Zhao, Yejing Wang, Zijian Zhang, Feng Tian, and Yefeng Zheng. Large language models enhanced sequential recommendation for long-tail user and item. *CoRR*, abs/2405.20646, 2024.
- [Luo *et al.*, 2021] Yingtao Luo, Qiang Liu, and Zhaocheng Liu. STAN: spatio-temporal attention network for next location recommendation. In *WWW*, pages 2177–2185. ACM / IW3C2, 2021.
- [Radford *et al.*, 2021] Alec Radford, Jong Wook Kim, Chris Hallacy, Aditya Ramesh, Gabriel Goh, Sandhini Agarwal, Girish Sastry, Amanda Askell, Pamela Mishkin, Jack

- Clark, Gretchen Krueger, and Ilya Sutskever. Learning transferable visual models from natural language supervision. In *Proceedings of the 38th International Conference on Machine Learning*, volume 139 of *Proceedings of Machine Learning Research*, pages 8748–8763. PMLR, 2021.
- [Rao *et al.*, 2022] Xuan Rao, Lisi Chen, Yong Liu, Shuo Shang, Bin Yao, and Peng Han. Graph-flashback network for next location recommendation. In *The 28th ACM SIGKDD Conference on Knowledge Discovery and Data Mining*, pages 1463–1471. ACM, 2022.
- [Rendle *et al.*, 2010] Steffen Rendle, Christoph Freudenthaler, and Lars Schmidt-Thieme. Factorizing personalized markov chains for next-basket recommendation. In *Proceedings of the 19th International Conference on World Wide Web*, pages 811–820. ACM, 2010.
- [Roberts *et al.*, 2023] Jonathan Roberts, Timo Lüddecke, Sowmen Das, Kai Han, and Samuel Albanie. GPT4GEO: how a language model sees the world’s geography. *CoRR*, abs/2306.00020, 2023.
- [Sun *et al.*, 2020] Ke Sun, Tiejun Qian, Tong Chen, Yile Liang, Quoc Viet Hung Nguyen, and Hongzhi Yin. Where to go next: Modeling long- and short-term user preferences for point-of-interest recommendation. In *AAAI*, pages 214–221. AAAI Press, 2020.
- [Tang *et al.*, 2024] Jiabin Tang, Yuhao Yang, Wei Wei, Lei Shi, Lixin Su, Suqi Cheng, Dawei Yin, and Chao Huang. Graphgpt: Graph instruction tuning for large language models. In *SIGIR*, pages 491–500. ACM, 2024.
- [Touvron *et al.*, 2023] Hugo Touvron, Louis Martin, Kevin Stone, Peter Albert, Amjad Almahairi, and et. Llama 2: Open foundation and fine-tuned chat models. *CoRR*, abs/2307.09288, 2023.
- [Wang *et al.*, 2024] Shirui Wang, Bohan Xie, Ling Ding, Xiaoying Gao, Jianting Chen, and Yang Xiang. Secor: Aligning semantic and collaborative representations by large language models for next-point-of-interest recommendations. In *Proceedings of the 18th ACM Conference on Recommender Systems, RecSys*, pages 1–11. ACM, 2024.
- [Wei *et al.*, 2024] Wei Wei, Xubin Ren, Jiabin Tang, Qinyong Wang, Lixin Su, Suqi Cheng, Junfeng Wang, Dawei Yin, and Chao Huang. Llmrec: Large language models with graph augmentation for recommendation. In *Proceedings of the 17th ACM International Conference on Web Search and Data Mining*, pages 806–815. ACM, 2024.
- [Wu *et al.*, 2022] Yuxia Wu, Ke Li, Guoshuai Zhao, and Xueming Qian. Personalized long- and short-term preference learning for next POI recommendation. *IEEE Trans. Knowl. Data Eng.*, 34(4):1944–1957, 2022.
- [Wu *et al.*, 2024] Junda Wu, Cheng-Chun Chang, Tong Yu, Zhankui He, Jianing Wang, Yupeng Hou, and Julian J. McAuley. Coral: Collaborative retrieval-augmented large language models improve long-tail recommendation. In *Proceedings of the 30th ACM SIGKDD Conference on Knowledge Discovery and Data Mining*, pages 3391–3401. ACM, 2024.
- [Yan *et al.*, 2023] Xiaodong Yan, Tengwei Song, Yifeng Jiao, Jianshan He, Jiaotuan Wang, Ruopeng Li, and Wei Chu. Spatio-temporal hypergraph learning for next POI recommendation. In *SIGIR*, pages 403–412. ACM, 2023.
- [Yang *et al.*, 2015] Dingqi Yang, Daqing Zhang, Vincent W. Zheng, and Zhiyong Yu. Modeling user activity preference by leveraging user spatial temporal characteristics in lbsns. *IEEE Trans. Syst. Man Cybern. Syst.*, 45(1):129–142, 2015.
- [Yang *et al.*, 2022] Song Yang, Jiamou Liu, and Kaiqi Zhao. Getnext: Trajectory flow map enhanced transformer for next POI recommendation. In *SIGIR*, pages 1144–1153. ACM, 2022.
- [Yin *et al.*, 2023] Feiyu Yin, Yong Liu, Zhiqi Shen, Lisi Chen, Shuo Shang, and Peng Han. Next POI recommendation with dynamic graph and explicit dependency. In *AAAI*, pages 4827–4834. AAAI Press, 2023.
- [Zhang *et al.*, 2022] Lu Zhang, Zhu Sun, Ziqing Wu, Jie Zhang, Yew Soon Ong, and Xinghua Qu. Next point-of-interest recommendation with inferring multi-step future preferences. In *IJCAI*, pages 3751–3757. ijcai.org, 2022.
- [Zhang *et al.*, 2023] Yang Zhang, Fuli Feng, Jizhi Zhang, Keqin Bao, Qifan Wang, and Xiangnan He. Collm: Integrating collaborative embeddings into large language models for recommendation. *CoRR*, abs/2310.19488, 2023.
- [Zhang *et al.*, 2024] Dabin Zhang, Meng Chen, Weiming Huang, Yongshun Gong, and Kai Zhao. Exploring urban semantics: A multimodal model for POI semantic annotation with street view images and place names. In *IJCAI*, pages 2533–2541. ijcai.org, 2024.
- [Zhao *et al.*, 2022] Pengpeng Zhao, Anjing Luo, Yanchi Liu, Jiajie Xu, Zhixu Li, Fuzhen Zhuang, Victor S. Sheng, and Xiaofang Zhou. Where to go next: A spatio-temporal gated network for next POI recommendation. *IEEE Trans. Knowl. Data Eng.*, 34(5):2512–2524, 2022.